References

BORN, M. & HUANG, K. (1954). *Dynamical Theory of Crystal Lattices*. Oxford: Clarendon Press.

BOYSEN, H. (1977). *Untersuchungen an den strukturellen Phasenübergängen des K_2SnCl_6 mit Hilfe von Neutronenbeugungsmethoden*. Dissertation, Univ. München.

BOYSEN, H. & HEWAT, A. W. (1978). *Acta Cryst.* B**34**, 1412–1418.

BOYSEN, H., IHRINGER, J., PRANDL, W. & YELON, W. (1976). *Solid State Commun.* **30**, 1019–1024.

CHODOS, S. L. & SATTEN, R. A. (1975). *J. Chem. Phys.* **62**, 2411.

CRUICKSHANK, D. W. J. (1956). *Acta Cryst.* **9**, 757.

D'ANS-LAX (1970). *Taschenbuch für Chemiker und Physiker*, Vol. III. Berlin: Springer-Verlag.

DÉNOYER, F. (1977). *Etude des Transitions de Phase Structurale de $NaNbO_3$ par les Rayons X et Diffusion Inélastique des Neutrons*. Thesis, Univ. Paris-Sud, Centre d'Orsay, France.

DÉNOYER, F., COMÈS, R., LAMBERT, M. & GUINIER, A. (1974). *Acta Cryst.* A**30**, 423–430.

EWALD, P. P. (1921). *Ann. Phys.* **64**, 250.

IHRINGER, J. (1977). *Röntgenographische Untersuchungen der Hochtemperaturstruktur und der Phasenumwandlungen von K_2SnCl_6*. Dissertation, Univ. München.

International Tables for X-ray Crystallography (1974). Vol. IV. Birmingham: Kynoch Press.

JEFFREY, K. R. (1972). *J. Magn. Reson.* **7**, 184–195.

KUGLER, W. (1979). Private communication and to be published.

LEIBFRIED, G. (1955). *Encyclopedia of Physics*, Vol. 7, part 1, edited by S. FLÜGGE, p. 132. Berlin: Springer-Verlag.

LERBSCHER, J. A. & TROTTER, J. (1976). *Acta Cryst.* B**32**, 2671–2672.

LYNN, J. W., PATTERSON, H. H., SHIRANE, G. & WHEELER, R. G. (1978). *Solid State Commun.* **27**, 859.

MARADUDIN, A. A. & VOSKO, S. H. (1968). *Rev. Mod. Phys.* **40**, 1.

MORFEE, R. G. S., STAVELEY, L. A. K., WALTERS, S. T. & WIGLEY, D. L. (1960). *J. Phys. Chem. Solids*, **13**, 132–144.

O'LEARY, G. P. & WHEELER, R. G. (1970). *Phys. Rev. B*, **1**, 4409.

PATTERSON, H. H. & LYNN, J. W. (1979). Submitted for publication.

SASANE, A., NAKAMURA, D. & KUBO, M. (1970). *J. Magn. Reson.* **3**, 76–83.

SHELDRICK, G. M. (1975). *SHELX – version of June 75*. University Chemical Laboratory, Lensfield Road, Cambridge, England.

VOGT, K. (1979). Private communication and to be published.

WINTER, J., RÖSSLER, K., BOLZ, J. & PELZL, J. (1976). *Phys. Status Solidi*, **74**, 193–198.

Acta Cryst. (1980). A**36**, 96–103

An Electron Diffraction Study of the Molecular Structure of the Sodium Chloride Dimer

BY H. MIKI, K. KAKUMOTO,* T. INO, S. KODERA AND J. KAKINOKI†

Department of Physics, Faculty of Science, Osaka City University, Sugimoto-cho, Sumiyoshi-ku, Osaka 558, *Japan*

(*Received* 29 *May* 1978; *accepted* 7 *August* 1979)

Abstract

The structure of sodium chloride has been studied by gas-phase electron diffraction using photographic plates designed for high-temperature work [Kakumoto, Ino, Kodera & Kakinoki (1977). *J. Appl. Cryst.* **10**, 100–103]. The molecular structure at about 1130 K has been determined by an analysis based on the new complex scattering factors for Na^+ and Cl^- calculated recently by the present authors. The radial distribution function shows the existence of a considerable amount of dimer molecules in the vapor. The structures of the monomer and dimer have been analyzed by a least-squares method assuming that the dimer is of a planar diamond shape: for monomer r_a(Na–Cl) = 2·392 ± 0·028, for dimer r_a(Na–Cl) = 2·515 ± 0·017, r_a(Cl–Cl) = 3·893 ± 0·021 Å, ∠ClNaCl = 101·4 ± 0·8°. The present study indicates that the Na–Cl distance of the dimer is longer than that of the monomer and the determined structure parameters differ appreciably from existing theoretical predictions.

Introduction

The structure of alkali halide molecules at high temperatures was studied by electron diffraction for the first time by Maxwell, Hendricks & Mosley (1937). They determined the internuclear distances in various

* Present address: Koyo Research Center, Kokubu, Kashiwara-shi, Osaka 582, Japan.

† Present address: Setsunan University, Ikeda-naka, Neyagawa-shi, Osaka 572, Japan.

0567-7394/80/010096-08$01.00

diatomic molecules but did not consider the possibility that the molecules contained dimers or other polymers.

Bauer, Ino & Porter (1960) determined the molecular structure of lithium chloride dimer at 1093 K by electron diffraction. This temperature was nearly the upper limit for their apparatus, because at higher temperatures the photographic plate was blackened by extraneous radiation from the sample oven. Akishin & Rambidi (1960) protected their photographic emulsion by coating the surface with indian ink and determined the dimer structure of lithium bromide and iodide. Structures of various other vapors were studied by this method (Akishin, Rambidi & Spiridonov, 1967; Tolmachev & Rambidi, 1973). The dimer structure of sodium chloride has been predicted theoretically (Berkowitz, 1958; Milne & Cubicciotti, 1958; Akishin & Rambidi, 1960; Trugman & Gordon, 1976), but it has never been determined experimentally. This is probably due to the difficulty in obtaining well-defined halo patterns at a temperature as high as 1130 K. However, a new technique of covering the photographic plate with aluminium foil has made it possible to get well-defined halo patterns without fogging, even at 2800 K (Kakumoto, Ino, Kodera & Kakinoki, 1977). In the present paper, the diffraction pattern of sodium chloride vapor obtained on this type of plate is analyzed.

The theory of molecular scattering used in the analysis of gas-phase structure assumes that each electron is scattered by only one atom in the molecule. Since the atoms in sodium chloride are considered to be highly ionized, it seems more desirable to use complex atomic scattering factors for Na^+ and Cl^- than those for the neutral atoms. In the present study, independent analyses, I and II, are made on the basis of the factors for the neutral atoms (*International Tables for X-ray Crystallography*, 1974) and of those for the atomic ions calculated recently (Miki, Ohsaki, Ino, Hata & Sakai, 1979), respectively. The structures of the monomer and the dimer determined by these analyses are reported.

Experimental

The sample of sodium chloride was a special-grade reagent with purity higher than 99·9%. An electron diffraction camera with an r^3 rotating sector (Ino, 1953) was operated at 55·8 kV, and diffraction patterns were recorded with plate-to-nozzle distances of 180·8 and 375·6 mm. The range of scattering angles covered corresponds to $s_{min} = 2$ and $s_{max} = 17$ Å^{-1}, where $s = (4\pi/\lambda)\sin(\psi/2)$, ψ being the scattering angle. The photographic plates designed for high-temperature work were prepared from a Kodak Electron Image Plate by the procedure given by Kakumoto, Ino, Kodera & Kakinoki (1977).

The oven was similar to that designed by Bauer, Ino & Porter (1960). A schematic diagram is shown in Fig. 1. The sample container, 10 mm in diameter and 40 mm in height, and a cone-shaped nozzle were made of inconel. They were heated by radiation or electron bombardment from a pair of *V*-shaped thoriated tungsten filaments, which were arranged symmetrically to minimize the influence of the electromagnetic field caused by the currents on the electron beam. The temperature of the nozzle and that of the lower part of the sample container were measured by two Pt/Pt–13% Rh thermocouples as shown in Fig. 1. The temperature of the nozzle was 20 K higher than that of the lower part of the sample container. The temperature of the sample container was adjusted to 1130 K (estimated from Chandrasekharaiah, 1967) so as to get a vapor pressure of about 70 Pa. The nozzle and the container were surrounded by three radiation shields made of molybdenum; the innermost shield was set at a negative voltage equal to that of the filaments, while the outer two were set at ground potential (Akishin, Rambidi & Spiridonov, 1967).

The oven was set in the camera and its position was adjusted with screw spacers so as to set the tip of the nozzle 0·5 mm from the electron beam. The vapor emitted from the nozzle was condensed on a copper trap with a liquid-nitrogen tank and the walls of the apparatus surrounding the vaporizer were water-cooled.

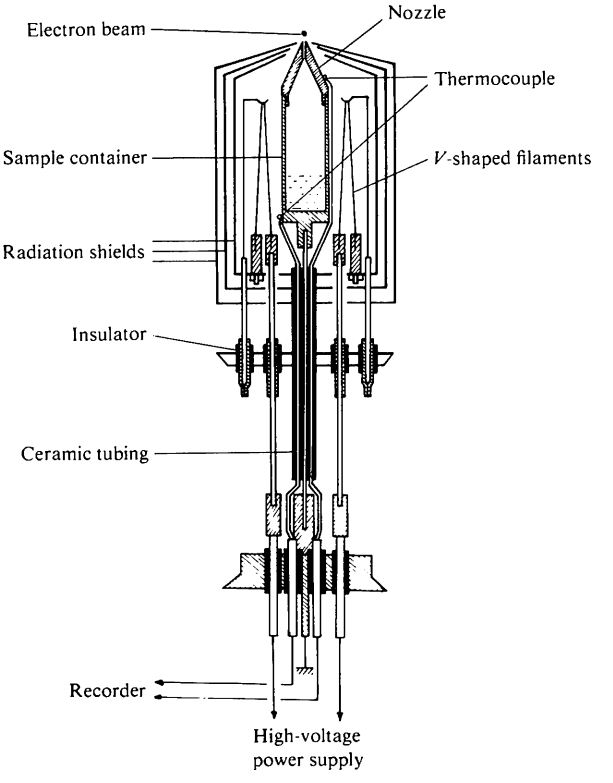

Fig. 1. Schematic diagram of the oven.

The optical density of the plate was measured by a recording densitometer system. The plates were rotated at 200–400 r/min during the scan across the diameter of the halos in order to reduce noise.

The photographic characteristics of the Al-covered plates have been described (Kakumoto, Ino, Kodera & Kakinoki, 1977). Three plates with short and three plates with long camera distance were selected from sixteen plates and analyzed.

Radial distribution analysis

At temperatures around 1130 K, the amplitudes of thermal vibrations for internuclear distances are so large that the oscillations in the intensity due to the molecular term cannot be detected beyond $s = 15$ Å^{-1}, as shown in Fig. 2. As a result, a constant ratio of the observed background intensity to the theoretical background, I_{bg}, was found in the range $s = 15$–17 Å^{-1}:

$$I_{bg} = |f_{Na}|^2 + |f_{Cl}|^2 + 4(S_{Na} + S_{Cl})/a_0^2 s^2, \quad (1)$$

where f is the complex atomic scattering factor for electrons, S is the incoherent atomic scattering factor for X-rays (*International Tables for X-ray Crystallography*, 1974) and $a_0 = h^2/(4\pi^2 me^2)$. By curve fitting at several points in this region, the scale factor for the normalization of observed intensity was obtained. From the normalized observed intensity, I_{tot}, the experimental molecular term, M_{exp}, was derived as

$$M_{exp} = (I_{tot} - I_{bg})/I_{atm}, \quad (2)$$

where $I_{atm} = |f_{Na}|^2 + |f_{Cl}|^2$. In terms of the effective internuclear distance, r_a, the effective mean-square amplitude of vibration, l, and the phase parameter, κ, the molecular term is expressed as (Kuchitsu, 1967)

$$M_{the}(s) = \sum_{ij} A_{ij}\mu_{ij}(s)e^{-l_{ij}^2 s^2/2} \times \{\sin[s(r_{aij} - \kappa_{ij}s^2)]\}/sr_{aij}, \quad (3)$$

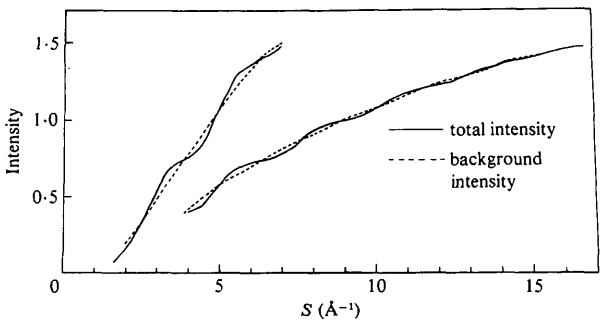

Fig. 2. The observed total intensity and the refined background (in arbitrary units).

where

$$\mu_{ij}(s) = |f_i||f_j| \cos(\eta_i - \eta_j)/(|f_{Na}|^2 + |f_{Cl}|^2), \quad (4)$$

η_i is the phase of the complex scattering factor for the i atom and A_{ij} is a factor specified by both

$$X = \text{number of dimers/number of monomers} \quad (5)$$

and the number of the r_{ij} pairs in the monomer or dimer.

The atomic scattering factors for 55·8 keV electrons of Na and Cl are compared with those of Na^+ and Cl^- in Fig. 3. As seen in this figure and as stated by Miki *et al.* (1979), the scattering amplitudes of the neutral atoms and ions are almost the same except in the vicinity of $s = 0$ and the differences in the scattering phase η are nearly constant and $(\eta_{Na} - \eta_{Cl}) - (\eta_{Na^+} - \eta_{Cl^-}) \simeq 0{\cdot}379$ in the region of $s \geq 3$ Å^{-1}.

In the region $s \geq 3{\cdot}0$ Å^{-1}, where M_{exp} is used for the subsequent analysis, the differences between μ_{ij} and constants $C_{ij} = Z_i Z_j/(Z_{Na}^2 + Z_{Cl}^2)$ for the Na–Na

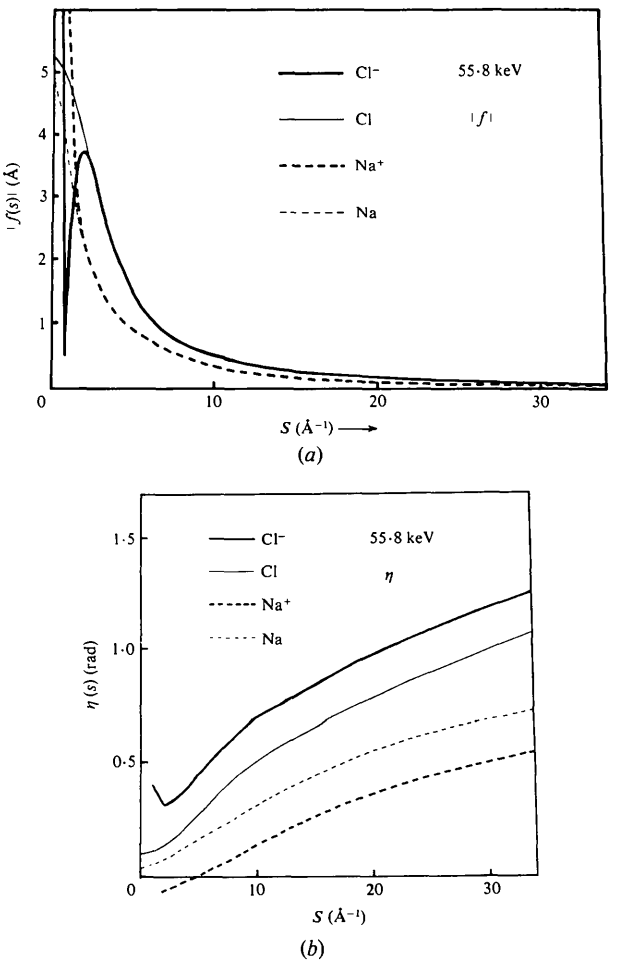

Fig. 3. The amplitudes $|f(s)|$ (*a*) and phases $\eta(s)$ (*b*) for the elastic scattering factors of Na and Cl neutral atoms and their ions for an incident electron energy of 55·8 keV.

and Cl—Cl pairs are negligible but a considerable difference for the Na—Cl pair is perceptible.

Since the intensity in the small s could not be observed because of the dead space of the sector, the radial distribution curve (RDF), $4\pi rD(r)$, was calculated in the usual manner as follows:

$$4\pi rD(r) = \frac{2}{\pi}\int_0^{s_{min}} sM_{cal}(s)\, e^{-\alpha^2 s^2} \sin(sr)\, ds + \frac{2}{\pi}\int_{s_{min}}^{s_{max}} sM_{exp}(s)\, e^{-\alpha^2 s^2} \sin(sr)\, ds, \quad (6)$$

where M_{cal} is a modified function of (3) with $\mu_{ij}(s)$ replaced by C_{ij} and $s_{min} = 3$, $s_{max} = 14$ Å^{-1} and $\alpha = 0{\cdot}11$. The integration was replaced by summation over evenly spaced s values with spacing $\Delta s = 0{\cdot}2$ Å^{-1}.

At an initial stage of the RDF calculation, the monomeric NaCl structure $r_e = 2{\cdot}3606$ Å, determined by microwave spectroscopy (Honig, Mandel, Stitch & Townes, 1954), was assumed to calculate the M_{cal} for $s \leq s_{min}$. Then the background and the trial structure model for a monomer–dimer mixture were refined by iteration using the non-negativity criterion for RDF (Karle & Karle, 1950). To check the validity of this criterion, non-negativity of a pair function, Q_{ij} (Warren, 1969), was confirmed for pairs of both neutral atoms and ions.

$$Q_{ij}(x) = \int_0^{s_{min}} C_{ij}\, e^{-\alpha^2 s^2} \cos(sx)\, ds + \int_{s_{min}}^{s_{max}} \mu_{ij}(s)\, e^{-\alpha^2 s^2} \cos(sx)\, ds, \quad (7)$$

where $x = r - r_{ij}$. The Q_{ij} curves for Na^+—Na^+, Na^+—Cl^- and Cl^-—Cl^- plotted in Fig. 4 show that negative parts are negligible in comparison with the peak height.

The final RDF curves obtained in analyses I and II are drawn in Fig. 5, where two separate peaks can be seen. This feature indicates the existence of a considerable amount of dimer molecules in the vapor. The final background was obtained with small corrections (less than 4%) of theoretical I_{bg}. Fig. 2 is a plot of one set of the observed intensity data for short and long camera distances. The final reduced intensity $M_{exp}(s)$ was obtained for each set of data and the average of the three sets is plotted in Fig. 6.*

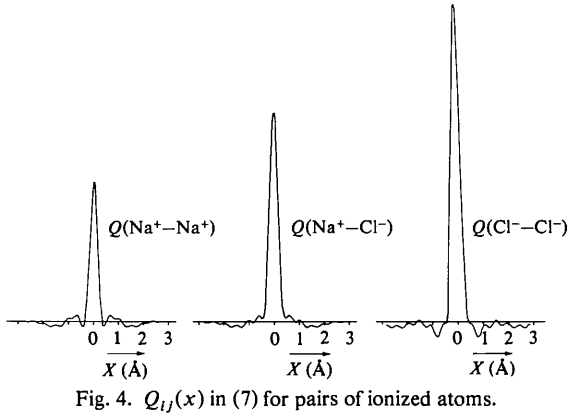

Fig. 4. $Q_{ij}(x)$ in (7) for pairs of ionized atoms.

Least-squares analysis

After a model was estimated by matching the theoretical RDF to the refined experimental RDF

* A list of the averaged $M_{exp}(s)$ has been deposited with the British Library Lending Division as Supplementary Publication No. SUP 34673 (2 pp.). Copies may be obtained through The Executive Secretary, International Union of Crystallography, 5 Abbey Square, Chester CH1 2HU, England.

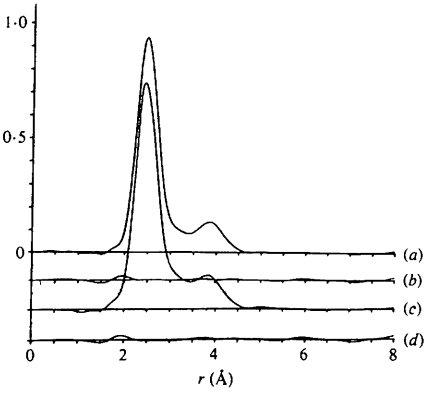

Fig. 5. The experimental RDF curves for analyses I and II and their differences from the best fit theoretical RDF. (*a*) RDF_{exp} for II; (*b*) $RDF_{exp} - RDF_{the}$ for II; (*c*) RDF_{exp} for I; (*d*) $RDF_{exp} - RDF_{the}$ for I.

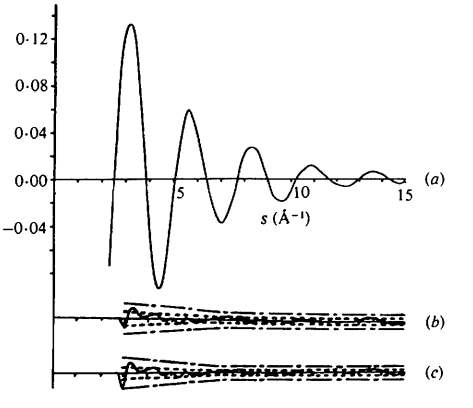

Fig. 6. The experimental reduced intensity $M_{exp}(s)$ and the deviations [solid lines in (*b*) and (*c*)] $M_{exp}(s) - M_{the}(s)$ in analyses II and I. In (*b*) and (*c*) the inner broken lines indicate the limit of sensitivity in photometry and the outer chain lines the limit of errors in $M_{exp}(s)$ estimated from three independent sets of data of reduced intensities.

curve, $sM_{exp}(s)$ was fitted at $s_m = m\Delta s$ ($\Delta s = 0{\cdot}2$, $15 \leq m \leq 68$) by a least-squares procedure, as outlined by Hedberg & Iwasaki (1964), so as to satisfy the approximate relation

$$sM_{exp}(s) = ksM_{the}(s), \tag{8}$$

where k is the index of resolution.

The weight for the least-squares analysis, P, was determined so as to represent the reliability of the reduced intensity at each point of s. Since errors of the photodensities were found to be nearly uniform and correlation among them caused by densitometry was considered to be negligible, P was chosen as a diagonal matrix whose diagonal elements were assumed to be proportional to the ratio of the densitometer reading to the reduced intensity.

The dimer molecule was assumed to be of a planar diamond shape in accordance with the models proposed by previous workers (O'Konski & Higuchi, 1955; Berkowitz, 1958; Milne & Cubicciotti, 1958; Bauer, Ino & Porter, 1960; Akishin & Rambidi, 1960; Akishin, Rambidi & Spiridonov, 1967; Trugman & Gordon, 1976). Hence, the bond distance of the dimer, r_a^d(Na—Cl), is expressed as

$$r_a^d(\text{Na—Cl}) = \tfrac{1}{2}[r_a^d(\text{Na—Na})^2 + r_a^d(\text{Cl—Cl})^2]^{1/2}. \tag{9}$$

A least-squares analysis was programmed to allow any of the following nine parameters to vary independently: r_a^m(Na—Cl), l^m(Na—Cl) corresponding to the monomer molecule; r_a^d(Na—Na), r_a^d(Cl—Cl), l^d(Na—Cl), l^d(Na—Na), l^d(Cl—Cl) corresponding to the dimer molecule, k and X defined in (8) and (5), respectively.

The phase parameters were fixed at approximate values estimated as follows: for the monomer molecule the phase parameter, κ^m(Na—Cl), was estimated as $1{\cdot}31 \times 10^{-4}$ Å^3 by the following formula (Kuchitsu, 1967)

$$\kappa = \tfrac{1}{6}al_h^4[1 + 8\chi/(1 + \chi)^2], \tag{10}$$

with $\chi = \exp(-hv_e/k_B T)$ and

$$l_h^2 = (h/8\pi^2 \mu v_e) \coth(hv_e/2k_B T), \tag{11}$$

where μ is the reduced mass; the characteristic frequency, v_e, was taken as 36·61 mm^{-1} (Rice & Klemperer, 1957) and the Morse parameter, a, was estimated to be 1·307 Å^{-1} (Honig, Mandel, Stitch & Townes, 1954).

For the dimer molecule the phase parameters were estimated by so-called diatomic approximation (Kuchitsu, 1967). If the potential functions for the bonded Na—Cl pair and the nonbonded Na—Na and Cl—Cl pairs are of Morse type, the phase parameter, κ, is represented by (10) as well as for the monomer. The so-called anharmonic stretching of the internuclear distance, $\langle \Delta r \rangle$, can be approximately expressed as (Kuchitsu, 1967)

$$\langle \Delta r \rangle = \tfrac{3}{2}al_h^2 \tag{12}$$

and so κ can be rewritten as

$$\kappa = \tfrac{1}{9}l_h^2[1 + 8\chi/(1 + \chi)^2]\langle \Delta r \rangle. \tag{13}$$

The effective characteristic frequencies for the Na—Cl, Na—Na and Cl—Cl pairs were determined by (11) from the estimated values of l^d(Na—Cl), l^d(Na—Na) and l^d(Cl—Cl), respectively. The Morse parameter, a, for the Na—Cl pair was estimated at 0·94 Å^{-1} by the following formula (Pauling & Wilson, 1935):

$$v_e = (a/2\pi)(2D/\mu)^{1/2}, \tag{14}$$

where D, corresponding to the bond energy of the Na—Cl bond, was assumed to be equal to that of the monomer molecule. Equations (10) and (12) gave κ^d(Na—Cl) = $3{\cdot}6 \times 10^{-4}$ Å^3 and $\langle \Delta r \rangle$(Na—Cl) = 0·039 Å. Geometrical relations among the bond lengths lead to the $\langle \Delta r \rangle$ value for the nonbonded pairs being approximated by (Konaka, Murata, Kuchitsu & Morino, 1966)

$$\langle \Delta r \rangle(\text{Na—Na}) = [2(1 + \cos\theta)]^{1/2}\langle \Delta r \rangle(\text{Na—Cl}), \tag{15}$$

$$\langle \Delta r \rangle(\text{Cl—Cl}) = [2(1 - \cos\theta)]^{1/2}\langle \Delta r \rangle(\text{Na—Cl}), \tag{16}$$

where θ designates $\angle$ClNaCl. Thus, the parameters κ^d(Na—Na) and κ^d(Cl—Cl) were estimated from (13) to be $5{\cdot}2 \times 10^{-4}$ and $9{\cdot}4 \times 10^{-4}$ A^3, respectively.

It was necessary to introduce several constraints in order to obtain convergence in the least-squares analysis. The error matrix showed that the matrix elements which represent the degree of correlation between the index of resolution and other parameters were significantly larger than the other matrix elements. Hence, the index of resolution, k, was first fixed at unity, and the distance parameter, r_{aij}, the amplitude of vibration, l_{ij}, and the ratio, X, were obtained as follows. Initial convergence was reached by constraining all the amplitudes of vibration at their values estimated from RDF, while varying the distance parameters and the ratio. Subsequently, these parameters were fixed at their best values and the amplitudes of vibration except for the Na—Na were allowed to vary. The values of r_{aij}, l_{ij} and X were obtained by iterating these cycles seven times. Then, the index of resolution, k, was allowed to vary, while r_{aij}, l_{ij} and X were fixed at their final values. Finally, the parameters for l_{ij} and k were fixed at their best values and the distance parameters, r_{aij}, and the ratio, X, were allowed to vary. The results of this least-squares analysis are listed in Table 1.

The estimation of experimental errors

Experimental errors for the observed parameters consist of both random errors and systematic errors.

Table 1. *Least-squares results of r_a, l and X and their standard deviations*

	Analysis I	Analysis II
Monomer		
r_a^m(Na–Cl) (Å)	2·396 ± 0·006	2·392 ± 0·010
Dimer		
r_a^d(Na–Cl)	2·538 ± 0·006	2·515 ± 0·005
r_a^d(Na–Na)	3·227 ± 0·013	3·184 ± 0·012
r_a^d(Cl–Cl)	3·917 ± 0·009	3·893 ± 0·008
∠ClNaCl (°)	101·0 ± 0·3	101·4 ± 0·2
The ratio X	0·50 ± 0·04	0·88 ± 0·08
Fixed values		
l^m(Na–Cl) (Å)	0·123	0·120
l^d(Na–Cl)	0·165	0·165
l^d(Na–Na)	0·18 (assumed)	0·18 (assumed)
l^d(Cl–Cl)	0·211	0·244
k	1·000	1·006

(1) *Random errors*

Random errors are introduced mainly in the processes of photography, development and photometry. These errors can be estimated from the standard deviation, σ, (in Table 1) in the least-squares treatment and from differences among the most probable values of the parameters obtained from three sets of plates (Morino, Kuchitsu & Murata, 1965). Since the latter differences were comparable with σ for almost all the parameters in this study, $2{\cdot}5\sigma$ was chosen as a measure of the random error.

(2) *Systematic errors*

In the present analysis, probable sources of systematic errors are drift of the accelerating voltage, uncertainty in the camera length, sample spread around the gas nozzle and uncertainty in the phase parameter, κ. The systematic errors are also listed inTable 2.

(*a*) *Error in the accelerating voltage.* The drift of the accelerating voltage was monitored during the experiment by measuring the primary voltage with a digital voltmeter. The drift was less than 0·3%. Therefore, this introduces error limits of less than 0·16% in the s scale or an error of less than $0{\cdot}0016r_a$ in the bond distances.

(*b*) *Error in the camera length.* Three photographic plates were set in a cassette so as to be perpendicular to the electron beam. Uncertainty in the camera length introduces a systematic error into the observed parameters. The errors of the $L\lambda$ measured from the Debye ring photographs of NaF deposits on a carbon film were 0·04% for the long camera length and 0·1% for the short camera length. Accordingly, the error limit is less than $0{\cdot}001r_a$ in the bond distances.

(*c*) *Errors due to sample spread around the nozzle.* A finite sample size causes an apparent decrease and increase in the bond distance and in the amplitude of thermal vibration, respectively. According to Morino & Murata (1965), an apparent change in r is determined by the density of gas molecules along the path of the primary electron beam as

$$\Delta r = -4r/\beta^2 L_0^2, \tag{17}$$

provided that the linear density $\rho(x)$ at a distance x measured along the electron beam from the intersection of the center line of the nozzle and the beam is expressed with a constant β as

$$\rho(x) = (\beta/2)\exp(-\beta x). \tag{18}$$

The β for the NaCl vapor in the present study was estimated at 0·6 mm^{-1} by the experimental procedure described in the Appendix. The errors of distances calculated from (17) for the short camera distance are listed in Table 2.

(*d*) *Errors due to the uncertainty in the phase parameter.* For the dimer molecule the κ values given in the preceeding section were estimated under the assumption that the D value for the Na–Cl pair in the dimer is the same as that in the monomer. Another assumption that the value of the Morse parameter, a, for the Na–Cl pair in the dimer is the same as that in the monomer, *i.e.* $a = 1{\cdot}307$ Å^{-1}, gives $4{\cdot}9 \times 10^{-4}$ Å^3 instead of $3{\cdot}6 \times 10^{-4}$ Å^3 as the κ value of the Na–Cl pair. The uncertainties in κ for pairs in the dimer were

Table 2. *Limits of error of r_a in analyses* I *and* II (Å)

Source of error		r_a^m(Na–Cl)	r_a^d(Na–Cl)	r_a^d(Na–Na)	r_a^d(Cl–Cl)
Random error ($2{\cdot}5\sigma$)	I	0·0158	0·0138	0·0333	0·0228
	II	0·0259	0·0123	0·0306	0·0195
Drift of voltage	I	0·0038	0·0041	0·0052	0·0063
	II	0·0038	0·0040	0·0051	0·0062
Camera length	I	0·0026	0·0028	0·0035	0·0043
	II	0·0026	0·0028	0·0035	0·0043
Vapor spread	I	0·0003	0·0003	0·0004	0·0005
	II	0·0003	0·0003	0·0004	0·0005
Uncertainty of κ	I	0·0070	0·0105	0·0310	0·0015
	II	0·0085	0·0105	0·0325	0·0010
Total error	I	0·0179	0·0180	0·0459	0·0241
	II	0·0276	0·0169	0·0451	0·0209

Table 3. *Comparison of the structure of* NaCl *dimer*

	Present work analysis II	Berkowitz (1958)	Milne & Cubicciotti (1958)	Akishin & Rambidi (1960)	Trugman & Gordon (1976)
NaCl dimer					
r(Na–Cl) (Å)	2·515 ± 0·017*	2·62	2·51	2·50	2·529
r(Na–Na)	3·184 ± 0·045	3·07	3·42	2·94	3·579
r(Cl–Cl)	3·893 ± 0·021	4·26	3·67	4·05	3·574
∠ClNaCl (°)	101·4 ± 0·8	108	94	108	89·9
NaCl monomer					
r(Na–Cl)	2·392 ± 0·028				
The ratio X	0·88 ± 0·20				

* Errors are derived from Table 2.

roughly estimated at $2{\cdot}3 \times 10^{-4}$ Å^3, that is the intermediate value in differences among the κ^d(Na–Cl) and the κ^m(Na–Cl). The errors of the distances due to this uncertainty were computed.

Total errors of r_a including all these errors are listed in the last rows in Table 2.

Results and discussion

The final results of the effective internuclear distance, r_a, derived from analysis II are listed in the second column of Table 3. In Fig. 6 the final experimental reduced-intensity curve M_{exp} (s) and its deviations from $M_{the}(s)$ calculated by (3) are shown. The experimental radial distribution curves are shown with deviations from the theoretical curves in Fig. 5. As seen in Tables 1 and 3, the structure parameters derived from analyses I and II agree within their error limits, though the X value estimated in II is considerably larger than that estimated in I. In comparison with the value of X = 0·33 estimated at 1130 K from the data obtained by Miller & Kusch (1956), the X value derived from I looks more reasonable than that from II. However, it is difficult to judge from the X values which analysis is more reasonable, because the dimer to monomer ratio in the vapor can differ from that in thermal equilibrium. As the Na–Cl bond in the monomer has 75% ionic character (Pauling, 1960) and the Na–Cl crystal has 94% (Kittel, 1976), the ionic character of the dimer is considered to be higher than that of the monomer. Consequently, from the view-point of current diffraction theory, II seems to be more acceptable than I, for the study on the structure of molecules so highly ionized.

As shown in Table 1, the effective internuclear distance in the monomer, r_a(Na–Cl) = 2·396 Å from I and 2·392 Å from II, is significantly longer than the internuclear distance, r_e = 2·3606 Å, derived from microwave spectroscopy.

The amplitude of vibration l^m(Na–Cl) for the monomer molecule obtained from (11) is about 0·12 Å at 1130 K. This value agrees well with the observed values in both analyses, 0·12 Å.

In Table 3, the theoretical values for the distances in the dimer are listed for comparison (Berkowitz, 1958; Milne & Cubicciotti, 1958; Akishin & Rambidi, 1960; Trugman & Gordon, 1976). The models used by Berkowitz, Milne & Cubicciotti and Akishin & Rambidi are ionic models based on a planar diamond shape and that used by Trugman & Gordon is an electron-gas model of the same shape. In spite of the experimental errors and the changes in the distances due to thermal deformation of the molecule, the discrepancies between the structure parameters determined in the present analyses and those calculated seem to be significant.

Experimentally, Akishin, Rambidi & Spiridonov (1967) determined only the internuclear distance of the Na–Cl pair in the dimer molecule under the assumption that the dimer gave a damped sinusoidal intensity distribution. Their value, 2·45 Å, differs somewhat from 2·538 ± 0·018 or 2·515 ± 0·017 Å determined in the present analyses.

The authors are indebted to Mr N. Minami for his fine cooperation in the computation in this work and to Dr T. Miura for his helpful suggestion for the dynamics of the vapor flow from the nozzle.

APPENDIX

In order to estimate the density distribution, $\rho(x)$, of the NaCl vapor in the present experiment, NaF vapor was chosen on account of its low hygroscopicity; the following experiment was carried out under a vacuum condition similar to that of the diffraction experiment. The vapor, whose pressure was about $1{\cdot}3 \times 10^2$ Pa in the container heated to 1400 K was emitted through the nozzle onto a cold glass plate placed at 1 and 2 mm

from the top of the nozzle. The distribution of the thickness of NaF condensed on the plate was measured by optical interference, where an equal-thickness fringe pattern of concentric rings was observed on the plate illuminated with the Na D line.

A study of vacuum evaporation onto a surface from a point source (Strong, 1958) showed that the thickness $f(x)$ of the film evaporated at a distance x measured along the plate from the center is given by the formula

$$f(x) \propto b(x^2 + b^2)^{-3/2}, \qquad (A1)$$

while the vapor density $\rho(x)$ is expressed as

$$\rho(x) \propto (x^2 + b^2)^{-1}$$

and

$$\rho(x) \propto f(x)/\cos\theta, \qquad (A2)$$

where b is the distance from the source to the plate and θ is the angle between the normal to the surface and the line connecting the surface with the source. The measured thickness distributions, $h(x)$, for plate distances of 1 and 2 mm were compared with $f(x)$ in $(A1)$ with $b = 1{\cdot}13$ and $2{\cdot}2$ mm, respectively. For example, $h(x)$ for the plate distance 1 mm and $f(x)$ with $b = 1{\cdot}13$ mm are shown in Fig. 7 by a thin, solid line and a broken line, respectively. Since the agreement between the two curves is good and the difference of $b = 1{\cdot}13$ mm from the measured distance $1{\cdot}0$ mm is small, the vapor flow near the nozzle was considered to be similar to the flow emitted from the center of the nozzle with an equal probability in all directions. Then, $\rho(x)$ was estimated as $h(x)/\cos\theta$, as shown by the thick solid line in Fig. 7. By fitting this $\rho(x)$ to (18), $\beta = 0{\cdot}6$ mm^{-1} was obtained.

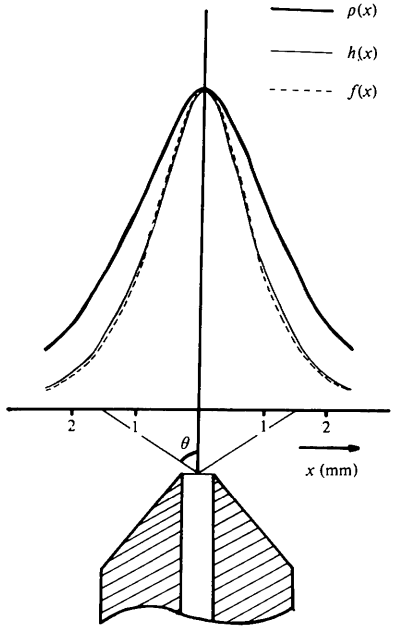

Fig. 7. The thickness distribution $h(x)$ of the film condensed on a glass plate at a nozzle-to-plate distance of $1{\cdot}0$ mm, $f(x)$ defined in $(A1)$ with $b = 1{\cdot}13$ mm and the vapor distribution $\rho(x)$ estimated along the path of the electron beam 1 mm from the nozzle. The vertical scales are arbitrary.

References

AKISHIN, P. A. & RAMBIDI, N. G. (1960). *Z. Phys. Chem.* **213**, 111–128.

AKISHIN, P. A., RAMBIDI, N. G. & SPIRIDONOV, V. P. (1967). *The Characterization of High-Temperature Vapors*, edited by J. L. MARGRAVE, pp. 300–358. New York: John Wiley.

BAUER, S. H., INO, T. & PORTER, R. F. (1960). *J. Chem. Phys.* **33**, 685–691.

BERKOWITZ, J. (1958). *J. Chem. Phys.* **29**, 1386–1394.

CHANDRASEKHARAIAH, M. S. (1967). *The Characterization of High-Temperature Vapors*, edited by J. L. MARGRAVE, pp. 495–507. New York: John Wiley.

HEDBERG, K. & IWASAKI, M. (1964). *Acta Cryst.* **17**, 529–537.

HONIG, A., MANDEL, M., STITCH, M. L. & TOWNES, C. H. (1954). *Phys. Rev.* **96**, 629–642.

INO, T. (1953). *J. Phys. Soc. Jpn*, **8**, 92–98.

International Tables for X-ray Crystallography (1974). Vol. IV, pp. 176–269. Birmingham: Kynoch Press.

KAKUMOTO, K., INO, T., KODERA, S. & KAKINOKI, J. (1977). *J. Appl. Cryst.* **10**, 100–103.

KARLE, J. & KARLE, I. L. (1950). *J. Chem. Phys.* **18**, 957–962.

KITTEL, C. (1976). *Introduction to Solid State Physics*, 5th ed., p. 95. New York: John Wiley.

KONAKA, S., MURATA, Y., KUCHITSU, K. & MORINO, Y. (1966). *Bull. Chem. Soc. Jpn*, **39**, 1134–1146.

KUCHITSU, K. (1967). *Bull. Chem. Soc. Jpn*, **17**, 498–504.

MAXWELL, L. R., HENDRICKS, S. B. & MOSLEY, V. M. (1937). *Phys. Rev.* **52**, 968–972.

MIKI, H., OHSAKI, H., INO, T., HATA, J. & SAKAI, M. (1979). In preparation.

MILLER, R. C. & KUSCH, P. (1956). *J. Chem. Phys.* **25**, 860–876.

MILNE, T. A. & CUBICCIOTTI, D. (1958). *J. Chem. Phys.* **29**, 846–851.

MORINO, Y., KUCHITSU, K. & MURATA, Y. (1965). *Acta Cryst.* **18**, 549–557.

MORINO, Y. & MURATA, Y. (1965). *Bull. Chem. Soc. Jpn*, **38**, 114–119.

O'KONSKI, C. T. & HIGUCHI, W. I. (1955). *J. Chem. Phys.* **23**, 1175–1176.

PAULING, L. (1960). *The Nature of The Chemical Bond*, 3rd ed., pp. 97–102. Cornell Univ. Press.

PAULING, L. & WILSON, E. B. (1935). *Introduction to Quantum Mechanics*, pp. 263–274. New York: McGraw-Hill.

RICE, S. A. & KLEMPERER, W. (1957). *J. Chem. Phys.* **27**, 573–579.

STRONG, J. (1958). *Procedures in Experimental Physics*, pp. 151–187. New Jersey: Prentice-Hall.

TOLMACHEV, S. M. & RAMBIDI, N. G. (1973). *High Temp. Sci.* **5**, 385–394.

TRUGMAN, S. & GORDON, R. G. (1976). *J. Chem. Phys.* **64**, 4625–4627.

WARREN, B. E. (1969). *X-ray Diffraction*, pp. 135–142. Massachusetts: Addison-Wesley.